# Surface Pressure of Charged Colloids at the Air/Water Interface

Aviv Karnieli,[†] Tomer Markovich,[†,‡] and David Andelman*,[†]

[†]Raymond and Beverly Sackler School of Physics and Astronomy, Tel Aviv University, Ramat Aviv 69978, Tel Aviv, Israel

[‡]DAMTP, Centre for Mathematical Sciences, University of Cambridge, Cambridge CB3 0WA, United Kingdom

**ABSTRACT:** Charged colloidal monolayers at the interface between water and air (or oil) are used in a large number of chemical, physical, and biological applications. Although considerable experimental and theoretical effort has been devoted in the past few decades to the investigation of such monolayers, some of their fundamental properties are not yet fully understood. In this article, we model charged colloidal monolayers as a continuum layer of finite thickness, with a separate charge distribution on the water and air sides. The electrostatic surface free energy and surface pressure are calculated via the charging method and within the Debye−Hückel approximation. We obtain the dependence of surface pressure on several system parameters: the monolayer thickness, its distinct dielectric permittivity, and the ionic strength of the aqueous subphase. The surface pressure scaling with the area per particle, $a$, is found to be between $a^{-2}$ in the close-packing limit and $a^{-5/2}$ in the loose-packing limit. In general, it is found that the surface pressure is strongly influenced by charges on the air side of the colloids. However, when the larger charge resides on the water side, a more subtle dependence on salt concentration emerges. This corrects a common assumption that the charges on the water side can always be neglected due to screening. Finally, using a single fit parameter, our theory is found to fit the experimental data well for strong- to intermediate-strength electrolytes. We postulate that an anomalous scaling of $a^{-3/2}$, recently observed in low ionic concentrations, cannot be accounted for within a linear theory, and its explanation requires a fully nonlinear analysis.
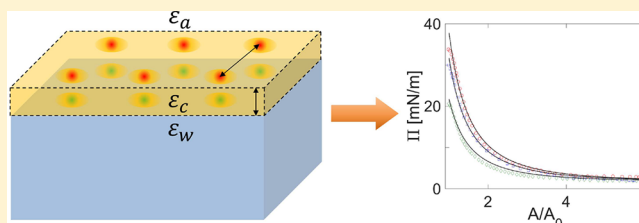
## INTRODUCTION

Molecular monolayers at the water/air or water/oil interfaces have been investigated intensively for more than a century, starting with the pioneering work of Langmuir and Blodgett.[1−7] They not only provide an important manifestation of the thermodynamics of two-dimensional systems but also equally offer several interesting applications in nanolithography, micropatterning, and optical coatings.[7−9]

Related systems are monolayers of colloidal particles deposited at fluid/fluid interfaces. Much interest in the latter systems followed the seminal work of Pieranski,[10] who found that submicrometer polystyrene spheres are trapped at the air/water interface and self-assemble into a triangular lattice due to electrostatic repulsive interactions. More recently, a wide range of studies, including the crystallization and aggregation of colloidal particles, have been performed on such monolayers.[11−14]

Another key property of colloidal monolayers is their surface pressure/area isotherm. Such quantitative knowledge allows for the direct control of particle spreading and self-assembling at the interface. The surface pressure can be used to fine tune the interparticle spacing when the monolayer is deposited from an aqueous solution.[15] Furthermore, from measurements of interparticle forces and the monolayer surface pressure, one can infer the magnitude of the effective colloidal charge,[16−19] as this quantity is otherwise hard to measure.

Several approaches have been suggested for calculating the surface pressure.[16,17,20−23] Levental *et al.*[20] and Biesheuvel and

Soestbergen[21] modeled a charged monolayer as a surface with a continuous and uniform charge density and calculated the *electrostatic* contribution to the surface pressure. Using the nonlinear Poisson−Boltzmann (PB) theory leads to a nonlinear expression for the surface pressure, $\Pi$, expressed in terms of hyperbolic functions. This result, when treated within the linearized PB theory (the Debye−Hückel theory, DH, valid for small zeta potentials), yields a surface pressure that scales with $a$, the average area per particle, as $\Pi \sim a^{-2}$. In the opposite limit of weak electrolytes, however, the scaling is found to be $\Pi \sim a^{-1}$.[20] Because the model is valid only for a uniform surface charge density, it is restricted to the close-packing limit of the colloids, where the monolayer surface charge can be considered to be approximately uniform.

In the other limit of large interparticle separation, Aveyard *et al.*[16] studied the surface pressure of a charged monolayer at the water/oil interface and calculated $\Pi$ using a superposition of interparticle forces. These forces can be explained as a consequence of trapped charges residing at the particle/oil surface (in contact with the oil phase), away from the oil/water interface. The charges induce opposite image charges inside the aqueous phase as a way to satisfy the dielectric discontinuous jump at the water/oil interface. The monolayer in the dilute limit can be treated as a dipolar layer and yields a surface pressure that scales as $\Pi \sim a^{-5/2}$. We note that the

same scaling law was found to be in agreement with their own experimental results.[16]

The model by Aveyard et al.[16] mentioned above does not take into account the bulk concentration of ions in the aqueous subphase and is a reasonable approximation only in the high-ionic-strength (hence screened) limit. Moreover, because the model does not explicitly consider the distinct value of the dielectric constant of the colloidal monolayer, the dependence of $\Pi$ on the Debye screening length and the monolayer dielectric constant has not been calculated.

Recently, Petkov et al.[17,18] measured the monolayer surface pressure, $\Pi$, for charged silica particles deposited at the air/water interface. They calculated $\Pi$ from the Maxwell stress tensor, employing the so-called *Bakker formula*.[24] The electrostatic field is assumed to vanish in the aqueous phase and was calculated in the air phase by postulating some specific ionic profiles. The surface charge density of each colloid and its accompanying screening were evaluated within a cell that is superimposed on a square lattice. In the large interparticle separation limit, it was found that the surface pressure scales as $\Pi \sim a^{-3/2}$.

This scaling was shown to be in good agreement with experimental data[17,18,25] measured either in the absence of salt or for weak electrolytes (using two fitting parameters). However, it contradicts the scaling law found in ref 16. Albeit there is agreement between the model and experiment, the model was not derived in a self-consistent fashion. In particular, the use of the Bakker formula cannot be justified because it relies on the homogeneity of the surface charge distribution and the ionic profiles were postulated a priori to have a preset form. In addition, the ansatz used to express the screening resembles the form of a typical solution in DH (strong electrolyte) theory, although the considered experimental regime (weak electrolytes) is clearly beyond the scope of this approximation.

Motivated by these different models that yield distinct scaling forms ($\Pi \sim a^{-\alpha}$, where $\alpha = 1, 2,$[20] $5/2,$[16] or $3/2$[17]), we present in this article a different, more fundamental self-consistent approach. The thermodynamic definition of the surface pressure is employed without the need to make any further assumptions other than using the linearized DH theory. Our calculation shows that for small interparticle separation the collective monolayer surface charge behaves as a continuum density and the surface pressure scales as $\Pi \sim a^{-2}$, in agreement with ref 20. For large separation, the colloids exhibit dipole-like behavior and the scaling becomes $\Pi \sim a^{-5/2}$, in agreement with the results in ref 16. In addition to the agreement with the two limiting scenarios of colloidal packing in previous works,[16,20] our model provides a general dependence on the entire area per particle range, $\Pi = \Pi(a)$. The theory derived herein also agrees well with available experimental data[16,25] within the DH regime.

The present study addresses a generalized setup in which the colloidal monolayer has a finite thickness and an arbitrary value of the effective dielectric constant. By generalizing previous works,[16−23] we allow the colloidal charge distribution to be different on the water side versus the air side of the monolayer. The surface pressure is obtained for any average intercolloidal distance and is found to depend differently on the monolayer permittivity in the two limits of interparticle separation. Furthermore, the dependence on the salt concentration can become nonmonotonic for specific values of the charge density on the water side. This finding is in contrast with the commonly employed assumption that the pressure depends solely on the charge located on the air side of the colloids, for which the dielectric constant is much smaller, and when there is no screening.

## SURFACE PRESSURE OF A CHARGED INTERFACE

We present a general framework for calculating the surface pressure of an arbitrarily charged interface coupled to a bulk ionic solution. The definition of the surface tension, $\gamma$, is

$$\gamma = \left(\frac{\partial F}{\partial A}\right)_{T,V} \tag{1}$$

where $F$ is the free energy of the system (comprising an interface coupled to a bulk) and $A$ is the overall surface area.

The surface pressure is related to the change in surface tension. For a charged surface, we can compare the surface tension with and without the charges

$$\Pi = \gamma_0 - \gamma \equiv -\Delta\gamma_{el} \tag{2}$$

where $\gamma_0$ and $\gamma$ denote the surface tension in the absence and presence of surface charges, respectively. The electrostatic contribution to the surface pressure, $\Pi$, is expressed in terms of $\Delta f_{el}$, the change in the electrostatic surface free energy,

$$\Pi = -\left(\frac{\partial}{\partial A}\int_A \Delta f_{el}\ d^2r\right)_{T,V} \tag{3}$$

The surface free energy, $\Delta f_{el}$, is defined as the amount of work (per unit area) needed to *construct* the surface. We introduce now the spatially averaged surface free energy as

$$\langle\Delta f_{el}\rangle = \frac{1}{A}\int_A \Delta f_{el}\ d^2r \tag{4}$$

and via eq 3 write the surface pressure in terms of the mean area *per colloid* as $a \equiv A/N$, where $N$ is the number of colloidal particles on the surface,

$$\Pi = -\langle\Delta f_{el}\rangle - a\left(\frac{\partial\langle\Delta f_{el}\rangle}{\partial a}\right)_{T,V} \tag{5}$$

It is important to consider how the surface area is controlled in experiments. For a uniform surface charge density (for which $\langle\Delta f_{el}\rangle = \Delta f_{el}$), two fundamentally different situations can occur and are known as the *Gibbs monolayer* and the *Langmuir monolayer*.[5] For Gibbs monolayers, the particles are soluble in the aqueous subphase. The monolayer is an open system exchanging particles with the bulk such that the chemical potential remains fixed. For a charged monolayer, this means that when the monolayer expands or contracts its surface charge density remains constant because the underlying physical properties that determine the surface coverage, such as the adsorption energy per unit area, remain approximately fixed.[21,26,27] As a result, $\langle\Delta f_{el}\rangle$ is independent of the surface area and $\Pi = -\langle\Delta f_{el}\rangle$ by virtue of eq 5.

On the other hand, for Langmuir monolayers, the particles at the surface are completely insoluble in the water subphase, and the monolayer is a closed system with a fixed number of particles. The total monolayer charge, $Q = \int\sigma\ d^2r$, remains fixed, meaning that $\sigma \sim a^{-2}$, even when the monolayer undergoes expansion or compression. For a uniformly charged surface and within the linear DH theory, the surface free energy satisfies $\langle\Delta f_{el}\rangle \sim a^{-2}$, and from eq 5, $\Pi = \langle\Delta f_{el}\rangle$.

Although these two simple cases may seem similar at first glance, the Gibbs and Langmuir monolayers yield opposite relations between $\Pi$ and $\langle \Delta f_{el} \rangle$, as shown above. Clearly, these two extreme cases of *uniform* surface charge density are an oversimplification, and for nonuniform surface charge densities, the relation between $\Pi$ and $\langle \Delta f_{el} \rangle$ becomes more intricate.

In the present study, we consider only the case of insoluble Langmuir monolayers where the total charge $Q$ and particle number $N$ at the interface are constant but the charge density (per unit area) $\sigma$ can vary. The charged surface is coupled to an electrolyte solution, and $\Delta f_{el}$ is calculated using the Poisson–Boltzmann (PB) theory.[28,29] The water and air phases are treated as two continuum media with dielectric constants $\varepsilon_w$ and $\varepsilon_a$, respectively. The mobile ions in the aqueous solution are taken to be pointlike, yielding the well-known PB equation for a monovalent 1:1 electrolyte

$$\nabla^2 \psi = \frac{2en_b}{\varepsilon_0 \varepsilon_w} \sinh\left(\frac{e\psi}{k_B T}\right) \tag{6}$$

where $\psi$ is the electrostatic potential, $e$ is the elementary charge, $\varepsilon_0$ is the vacuum permittivity, $n_b$ is the bulk concentration of the electrolyte, and $k_B T$ is the thermal energy.

For an interface with surface charge $\sigma$ separating two media, the electrostatic boundary condition is

$$\hat{\mathbf{n}} \cdot [\varepsilon_r^- \nabla \psi^- - \varepsilon_r^+ \nabla \psi^+] = \frac{\sigma}{\varepsilon_0} \tag{7}$$

where $\hat{\mathbf{n}}$ denotes the unit vector normal to the surface. The $\pm$ superscripts on the potential and relative permittivity $\varepsilon_r$ of the media (e.g., $\varepsilon_a$, $\varepsilon_w$, etc.) denote the external (+) and internal (−) regions with respect to the surface, and the direction of $\hat{\mathbf{n}}$ is chosen to point from inside toward the outside.

From the well-known *charging method*,[28–30] the electrostatic free energy due to the presence of an electric double layer can be evaluated as

$$\Delta f_{el} = \int_0^\sigma \psi_s(\sigma') \, d\sigma' \tag{8}$$

Equations 4–8 are sufficient for obtaining the surface pressure in the most general case. (Although the above charging method takes into account the entropy of the mobile ions in the solution, it does not include the entropy of the surface charges. In our model, those charges originate from the charge distribution on large colloidal particles, forming a monolayer at the air/water interface, but because the colloids are considered to be macroparticles, this entropy contribution can be ignored.) However, for simplicity, the Debye–Hückel (DH) linearization scheme can be employed[28] for eq 6,

$$\nabla^2 \psi = \kappa_D^2 \psi \tag{9}$$

for cases in which $\psi \ll k_B T / e$. In eq 9, the inverse Debye screening length is $\kappa_D = \sqrt{8\pi l_B n_b}$, and the Bjerrum length $l_B = e^2 / (4\pi \varepsilon_0 \varepsilon_w k_B T)$ is about 0.7 nm in water ($\varepsilon_w \simeq 78$) at room temperature.

In the DH regime, $\psi_s$ and $\sigma$ are linearly related,[28,30] and eq 8 becomes

$$\Delta f_{el} = \frac{1}{2} \psi_s \sigma \tag{10}$$

This equation can be generalized for two charged surfaces, $S_i$, $i = 1, 2$, each with a surface potential $\psi_{s,i}$ and a surface charge $\sigma_i$,

$$\Delta f_{el} = \frac{1}{2} \sum_{i=1,2} \psi_{s,i} \, \sigma_i \tag{11}$$

Equation 11 is obtained by the linearization of the expression presented in ref 31 in the context of two interacting charged surfaces. In the following section, the above equation will be used to calculate the free energy for Langmuir monolayers, which are modeled as two charged interfaces separated by a dielectric layer (Figure 1b).
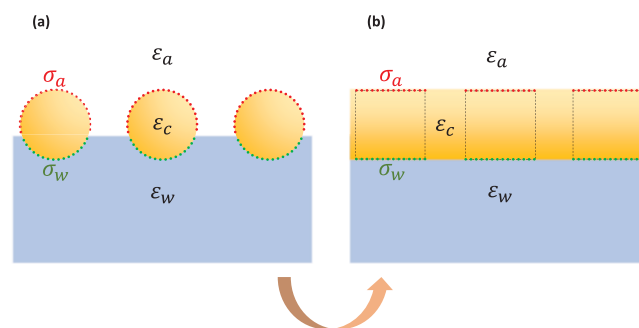


**Figure 1.** $\sigma_i$ and $\varepsilon_i$ refer to the surface charge on interface $i$ and permittivity in medium $i$, respectively. (a) Cross section of a colloidal monolayer at the air/water interface. Spherical colloids are partially immersed in the aqueous phase, with different charge distributions on their air- and water-facing sides. (b) Simplified model, where the colloids are now cubes with surface charges residing only on the air- and water-facing facets. The monolayer region has a uniform effective dielectric constant of $\varepsilon_c$.

## MODELING OF THE COLLOIDAL MONOLAYER

We first consider a model for a monolayer of charged colloidal particles at the air/water interface as presented in Figure 1a. Micrometer-sized colloids are modeled as dielectric spheres (of permittivity $\varepsilon_c$) partially submerged in the aqueous phase. Different charge distributions are present on the colloids' water- and air-facing surfaces, which, together with the ions in the electrolyte solution, give rise to the electrostatic interactions. Note that the colloids' finite-size dictates an excluded volume for the compression. This complex geometry, however, hinders the simplicity of our surface free-energy method.

The aforementioned setup can be greatly simplified when the partially immersed spherical colloids are modeled as dielectric cubes with the same dimensions, and the surface charges are now positioned on the water- and air-facing facets of the cubes (Figure 1b). Such an approximation recovers the main physical features. The redistribution of charge merely introduces geometric corrections (as was similarly approached in refs 17–19 and 32).

Moreover, we replace the dielectric constant as seen by the colloids with an effective permittivity of $\varepsilon_{eff}$ smeared over the monolayer region. This effective permittivity is comparable to the permittivity of the colloids and for simplicity is taken as $\varepsilon_{eff} = \varepsilon_c$. For the close packing of colloids, this represents a reasonable approximation. For loosely packed monolayers, we find that the interaction is dictated by dipole–dipole forces
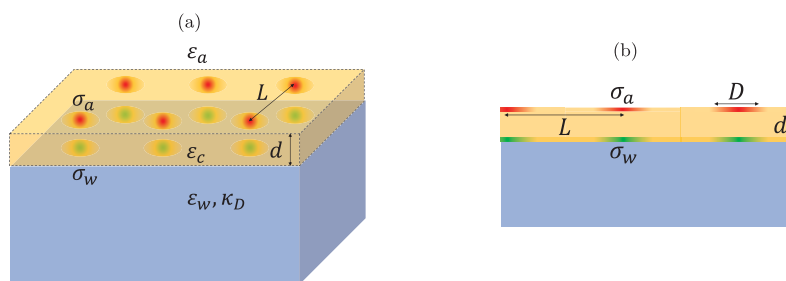
**Figure 2.** Schematic drawing of the colloidal monolayer in between two interfaces: a top one, at $z = 0$, in contact with air (dielectric constant $\varepsilon_a$), and a bottom one, at $z = -d$, in contact with an aqueous solution having a dielectric constant, $\varepsilon_w$, and a Debye screening length, $\kappa_D^{-1}$. (a) The layer of finite thickness, $d$, is modeled as a dielectric layer with dielectric constant $\varepsilon_c$ spread between the water and air phases. The colloidal charges accumulate on the water side and air side and form a square lattice with lattice constant $L$. The two corresponding surface charge densities are denoted, respectively, as $\sigma_a$ and $\sigma_w$. (b) Cross section of the monolayer. The colloid charge density is spread over the colloid diameter, $D$, and the distance between colloid centers is $L$.

mediated primarily through the *air* phase. The role played by $\varepsilon_{eff}$ is to merely determine the dipole strength, which is a local feature of the colloidal particle itself, consistent with our approximation $\varepsilon_{eff} = \varepsilon_c$.

The charged colloidal monolayer is schematically depicted in Figure 2. It is located at the interface between a dielectric medium of constant $\varepsilon_a$ (nonaqueous medium such as air or oil) on its top side and a monovalent 1:1 electrolyte solution of dielectric constant $\varepsilon_w$ on its bottom side. The colloidal monolayer medium is considered to be continuous with a finite thickness $d$ (we later set it equal to the colloid diameter, thus ignoring immersion in the aqueous phase due to wetting) and a dielectric constant $\varepsilon_c$. The charges residing on each side of a single colloid are modeled as a patch of surface charge (Figure 1). The charge distribution can take different values on the air-facing ($z = 0$) and water-facing ($z = -d$) sides.

The monolayer itself is constructed by repeating the pairs of surface charge patches (each representing an *individual* colloid) on a square lattice with lattice parameter $L$, as seen in Figure 2. Here, $L$ is the average distance between the colloids, which takes into account the colloids' excluded volume. Note that the patches can have an arbitrary shape and charge distribution on a typical length scale, $D < L$, which serves as an effective colloid diameter. For an arrangement on a square lattice, the total surface charge densities on the monolayer air side and water side, $\sigma_a(x, y)$ and $\sigma_w(x, y)$, become periodic functions in $x \to x + L$ and $y \to y + L$.

To calculate the surface pressure, we first need to evaluate the electrostatic potential. The potential in the air phase, $\psi^{(a)}$, as well as inside the colloidal monolayer region, $\psi^{(c)}$, satisfies the Laplace equation

$$\nabla^2 \psi^{(a)} = 0, \quad \nabla^2 \psi^{(c)} = 0 \tag{12}$$

while the potential in the aqueous phase, $\psi^{(w)}$, satisfies the DH equation, eq 9

$$\nabla^2 \psi^{(w)} = \kappa_D^2 \psi^{(w)} \tag{13}$$

and depends on the solution ionic strength via the Debye screening length, $\kappa_D^{-1}$.

The boundary conditions at the $z = 0$ and $z = -d$ planes are obtained from eq 7,

$$\varepsilon_c \frac{\partial \psi^{(c)}}{\partial z}\bigg|_{z=0^-} - \varepsilon_a \frac{\partial \psi^{(a)}}{\partial z}\bigg|_{z=0^+} = \frac{1}{\varepsilon_0}\sigma_a(x, y),$$

$$\varepsilon_w \frac{\partial \psi^{(w)}}{\partial z}\bigg|_{z=-d^-} - \varepsilon_c \frac{\partial \psi^{(c)}}{\partial z}\bigg|_{z=-d^+} = \frac{1}{\varepsilon_0}\sigma_w(x, y) \tag{14}$$

and at $z \to \pm\infty$, we demand that the electrostatic field vanishes, $\lim_{z\to\pm\infty} |\nabla\psi| = 0$.

## RESULTS

The surface free energy and pressure can be calculated (both numerically and analytically) by using the model periodicity and employing the Fourier transform on the surface charges and the electric potential. The two periodic charge densities, $\sigma_a(x, y)$ and $\sigma_w(x, y)$, are expressed by their Fourier series

$$\sigma_a(\mathbf{r}) = \frac{1}{L^2} \sum_{n,m=-\infty}^{\infty} \tilde{s}_a(\mathbf{k})e^{i\mathbf{k}\cdot\mathbf{r}},$$

$$\sigma_w(\mathbf{r}) = \frac{1}{L^2} \sum_{n,m=-\infty}^{\infty} \tilde{s}_w(\mathbf{k})e^{i\mathbf{k}\cdot\mathbf{r}} \tag{15}$$

where $\mathbf{r} = (x, y)$ is the in-plane vector. For a square lattice, integer numbers $\{n, m\} = 0, \pm 1, \pm 2...$, parametrize the discrete $\mathbf{k}$-vector of the reciprocal space with $\mathbf{k} = 2\pi/\left(L\sqrt{n^2 + m^2}\right)$, and $\tilde{s}_i(\mathbf{k})$ ($i$ = a, w) is the $\mathbf{k}$-component of the Fourier transform of a *single* colloid charge distribution. In a manner similar to eq 15, the surface potentials evaluated at the top and bottom surfaces, $\psi_s^{(a)}$ and $\psi_s^{(w)}$, can also be written in terms of their Fourier components

$$\psi_s^{(i)}(\mathbf{r}) = \sum_{n,m=-\infty}^{\infty} \tilde{\psi}_s^{(i)}(\mathbf{k})e^{i\mathbf{k}\cdot\mathbf{r}} \tag{16}$$

with $i$ = a, w and $\tilde{\psi}_s^{(i)}(\mathbf{k})$ denoting the Fourier coefficients of $\psi_s^{(i)}(\mathbf{r})$.

A linear relation between the surface potential and surface charge density emerges from the boundary conditions as our model is linear. The generalized linear response is written in Fourier space as the product

$$\tilde{\Psi}_s(\mathbf{k}) = \frac{1}{L^2}\mathbf{C}^{-1}(\mathbf{k})\,\tilde{\Sigma}(\mathbf{k}) \tag{17}$$

where in compact notation $\tilde{\Psi}_s(\mathbf{k}) = (\tilde{\psi}_s^{(a)}(\mathbf{k}), \tilde{\psi}_s^{(w)}(\mathbf{k}))$ and $\tilde{\Sigma}(\mathbf{k}) = (\tilde{s}_a(\mathbf{k}), \tilde{s}_w(\mathbf{k}))$ are vectors and $\mathbf{C}(\mathbf{k})$ is a $2 \times 2$ matrix. The diagonal components of the $\mathbf{C}(\mathbf{k})$ matrix are the differential capacitances (per unit area) of the 'a' and 'w' surfaces, while the off-diagonal components represent cross-capacitance terms between the two surfaces. One can then write $\langle \Delta f_{el} \rangle$ as a function of the inverse capacitance and the surface charge by using eq 11 and Parseval's theorem,

$$\langle \Delta f_{el} \rangle = \frac{1}{2L^4} \sum_{\mathbf{k}} \tilde{\Sigma} \mathbf{C}^{-1} \tilde{\Sigma} \tag{18}$$

Because $\langle \Delta f_{el} \rangle$ depends explicitly on the area per colloid $a = L^2$, eq 5 can be employed to calculate the surface pressure (details in Appendix A).

The quantities appearing in eq 18 are all obtained from the explicit solution of the boundary value problem defined in "Modeling of the colloidal monolayer" Section for the electrostatic potential (details in Appendix A). To obtain the potential, the boundary conditions (i.e., the surface charge distributions) must be specified. Here, we assume that this charge distribution is Gaussian, with separate values on the air (a) and water (w) sides of the monolayer

$$s(r) = \frac{2Q}{\pi D^2} \exp\left(-\frac{2r^2}{D^2}\right) \tag{19}$$

where $r = |\mathbf{r}|$, and $Q = Q_a$ or $Q_w$ is the charge on the 'a' or 'w' side, respectively. The limiting values for the surface pressure, however, remain independent of this specific choice of profile.

**Close-Packing Colloid Limit, $L \rightarrow D$.** In the close-packing limit, the interparticle spacing $L$ approaches the colloid effective diameter $D$. In this case, the limiting value of the surface pressure $\Pi$ can be derived analytically (details in Appendix A)

$$\Pi \simeq \left[ \frac{Q_a^2 d}{2\varepsilon_c \varepsilon_0} + \frac{(Q_a + Q_w)^2}{2\varepsilon_0 \varepsilon_w \kappa_D} \right] \frac{1}{a^2} \tag{20}$$

where $a \equiv L^2$ is the area per colloid. Therefore, in the close-packing limit $\Pi$ scales as $a^{-2}$ and is consistent with the continuum limit of the monolayer surface charge. As the colloids approach each other, their double layers overlap and resemble the response to a uniform surface charge density at the air/water interface. Note that eq 20 is independent of the specific surface charge distribution, $s(\mathbf{r})$, of each colloid.

**Dilute Colloid Limit, $L \gg D$.** The opposite regime of interparticle separation is the dilute limit, where $L \gg D$. A closed-form analytical expression for $\Pi$ can be derived by using the Euler−Maclaurin formula (details in Appendix A). The result obtained suggests that the surface pressure originates from dipolar interactions between the colloids

$$\Pi = \frac{\pi}{12} \frac{p_{eff}^2}{\varepsilon_0 \varepsilon_a} \frac{1}{a^{5/2}} + O\left(\frac{1}{a^{7/2}}\right) \tag{21}$$

where the effective dipole moment $p_{eff}$ is written as the sum of two terms,

$$p_{eff} = p_1 + p_2 = \frac{2\varepsilon_a}{\varepsilon_c} Q_a d + \frac{2\varepsilon_a}{\varepsilon_w} \frac{Q_a + Q_w}{\kappa_D} \tag{22}$$

In Appendix B, we calculate $\Pi$ directly from an effective model of dipole−dipole interactions and arrive at an identical result. This approach suggests that the dilute limit, as in eqs 21

and 22, is independent of the specific functional form of the surface charge density. One might indeed expect this behavior because the interparticle distance satisfies $D \ll L$ and the details of the colloidal charge distribution are washed out.

We note that there are two separate cases for the effective dipole moment, eq 22:

(i) In the case of strong electrolytes, where $\kappa_D d \gg [1 + (Q_w/Q_a)](\varepsilon_c/\varepsilon_w)$, $p_{eff}$ is approximated as

$$p_{eff} \simeq p_1 = \frac{2\varepsilon_a}{\varepsilon_c} Q_a d \tag{23}$$

and mainly depends on $p_1$ because the air-exposed charge induces an image charge in the aqueous phase at a distance of $2(\varepsilon_a/\varepsilon_c)d$.

(ii) In the case of weak electrolytes, namely, $\kappa_D d \ll [1 + (Q_w/Q_a)](\varepsilon_c/\varepsilon_w)$, $p_{eff}$ is well approximated by the second term, $p_2$,

$$p_{eff} \simeq p_2 = \frac{2\varepsilon_a}{\varepsilon_w} (Q_a + Q_w) \kappa_D^{-1} \tag{24}$$

The relevant charge determining the dipole moment is the net charge on both sides of the particle as a result of the electroneutrality due to screening. The charge separation is then proportional to the screening length.

For a given interparticle separation $L$, we express the dependence of $\Pi$ on the ionic strength using eqs 21 and 22,

$$\Pi = \left[ 1 + \left( 1 + \frac{Q_w}{Q_a} \right) \frac{\varepsilon_c}{\varepsilon_w} \frac{1}{\kappa_D d} \right]^2 \Pi_\infty \tag{25}$$

where $\Pi_\infty = \Pi(\kappa_D d \rightarrow \infty)$ is the surface pressure for a vanishing screening length. From eq 25, we deduce that for $Q_w/Q_a > 0$, $\Pi$ is a monotonic function of the Debye screening length and converges to $\Pi_\infty$ for very high electrolyte concentrations. However, if the ratio $Q_w/Q_a$ becomes negative, $\Pi$ might even vanish for certain values of $\kappa_D$, as can be seen in Figure 3 for a specific choice of $Q_w/Q_a = -100$. Moreover, $\Pi$ is nonmonotonic with respect to the salt concentration. This presents compelling evidence that surface charges on both sides of the colloid particle can play a role in determining the magnitude of $\Pi$. We shall discuss this observation further in the following sections.

**General Interparticle Separations.** The surface pressure, $\Pi$, can be calculated numerically for any intermediate value of interparticle separation $L$. In this case, it is most convenient to define a dimensionless parameter $\xi \equiv D/L$ where $0 < \xi \leq 1$, with $\xi \rightarrow 1$ denoting the close-packing limit and $\xi \ll 1$ denoting the dilute regime. We restrict ourselves to the more common case of strong electrolytes, $\kappa_D d \gg [1 + Q_w/Q_a] \times (\varepsilon_c/\varepsilon_w)$, with $Q_w = 0$, $d = D$, and $\kappa_D d = 10$. We have chosen $Q_w = 0$ on the water side, without a loss of generality, because it merely denotes the strong electrolyte regime as $\kappa_D d \gg \varepsilon_c/\varepsilon_w$.

The average electrostatic surface free energy, $\langle \Delta f_{el} \rangle$, is calculated by summing 100 terms of the two series in eq A4, where their explicit form is also given in Appendix A. $\Pi(\xi)$ is then evaluated via eq A5.

The quantities $\langle \Delta f_{el} \rangle$ and $\Pi$, rescaled by their maximal values at $\xi = 1$ ($\Pi_0$ and $\langle \Delta f_0 \rangle$, respectively), are shown in Figure 4 on a log−log plot. Clearly, both coincide in the close-packing limit ($\xi \lesssim 1$), where the continuum limit holds, i.e., $\Pi \simeq \langle \Delta f_{el} \rangle \sim \xi^4 \sim a^{-2}$. However, in the dilute regime ($\xi \ll 1$),
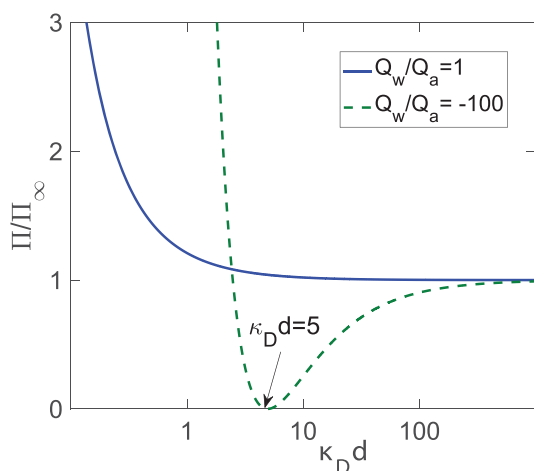
**Figure 3.** Rescaled surface pressure, $\Pi/\Pi_\infty$, for the dilute limit ($\xi \ll 1$) plotted as a function of the reduced screening parameter, $\kappa_D d$. The rescaling factor, $\Pi_\infty = \Pi(\kappa_D d \to \infty)$, is the pressure for strong electrolytes. Taking $\varepsilon_c = 4$ for silica particles and $\varepsilon_w = 80$, we compare the dependence on $\kappa_D d$ for two values of the charge ratio. For $Q_w/Q_a = 1$ (blue solid line), the dependence is monotonic and does not vanish, while for large negative ratios, $Q_w/Q_a = -100$ (dashed green line), the surface pressure is nonmonotonic and even vanishes for a certain value of $\kappa_D d$.
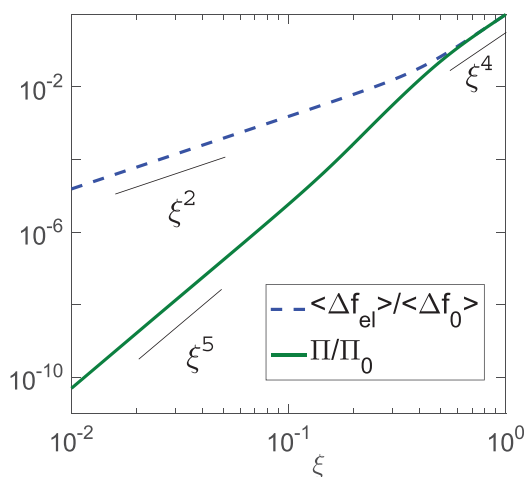


**Figure 4.** Rescaled surface pressure, $\Pi/\Pi_0$ (green solid line), and rescaled surface free energy, $\langle \Delta f_{el} \rangle / \langle \Delta f_0 \rangle$ (blue dashed line), plotted on a log–log plot as a function of $\xi = D/L$. The rescaling is done with respect to the close-packing values at $\xi = 1$. The free energy and pressure scale identically as $\sim \xi^4$ in the $\xi \to 1$ limit, where the monolayer can be regarded as having a uniform surface charge. In the dilute limit ($\xi \ll 1$), however, $\Pi \sim \xi^5$ and differs significantly from $\langle \Delta f_{el} \rangle \sim \xi^2$.

the surface free energy and surface pressure differ considerably as $\langle \Delta f_{el} \rangle \sim \xi^2 \sim a^{-1}$ and $\Pi \sim \xi^5 \sim a^{-5/2}$.

A plot of $\Pi$, rescaled by its maximal value, is given in Figure 5 for different values of the monolayer dielectric constant, $\varepsilon_c = 1, 2, 4,$ and 8. The variation of the rescaled surface pressure with $\varepsilon_c$ is quite substantial only in the dilute-packing limit, where it varies as $1/\varepsilon_c$, as is implied by eq A19. We note that $\Pi_0$ (the rescaling prefactor) is the close-packing value of $\Pi$, $\Pi_0 = \Pi(\xi = 1)$, and is by itself proportional to $1/\varepsilon_c$ (eq 20).
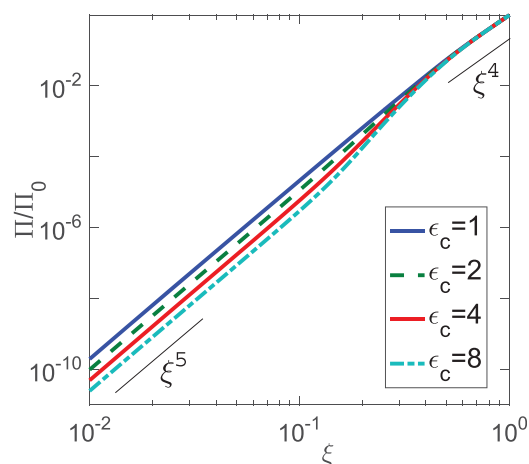


**Figure 5.** Log–log plot of the rescaled surface pressure, $\Pi/\Pi_0$, with $\Pi_0 = \Pi(\xi = 1)$, as a function of $\xi = D/L$ for different values of the monolayer dielectric constant, $\varepsilon_c = 1, 2, 4,$ and 8. Two scaling regimes of $\xi^5$ and $\xi^4$ can be seen, as in Figure 4. The rescaled surface pressure, $\Pi/\Pi_0$, does not show any dependence on $\varepsilon_c$ in the close-packing limit. In the dilute-packing limit, however, $\Pi/\Pi_0$ scales as $1/\varepsilon_c$.

## ■ COMPARISON TO EXPERIMENTS

It would be of value to compare our theoretical predictions to previous experiments. In refs 16 and 25, the surface pressure of charged polystyrene latex particles is measured at octane/water and decane/water interfaces, respectively. The fit to these experimental data shown in Figure 6 employs the full expression as prescribed in eqs A5 and A7−A9 and uses a single fit parameter, which is the air-exposed surface charge of a single colloid, $\sigma_a = Q_a/[\pi(D/2)^2]$.

In general, there are two fit parameters, $\sigma_a$ and $\sigma_w$. However, we observe that the experiments in refs 16 and 25 used intermediate to high salt concentrations. Thus, $\kappa_D^{-1} \leq 1$ nm is much smaller than the colloid particle size $D \geq 1$ $\mu$m, and $\varepsilon_a \ll \varepsilon_w$ for the two bounding media. It is then justified to neglect $\sigma_w$ because the contribution from the water charges becomes much smaller (details in Discussion section). We also find explicitly that employing $\sigma_w$ as a second fit parameter makes no substantial difference. Nevertheless, there might exist physical scenarios where the assumption $\sigma_w = 0$ is inaccurate (as is discussed below).

Figure 6a presents the fit with the data in ref 16. The data corresponds to an experimental setup with a 10 mM NaCl solution and particles of diameter $D = 2.6$ $\mu$m. The resulting air-exposed surface charge $\sigma_a$ is obtained as a fit parameter, $\sigma_a = 870$ $\mu$C/m$^2$ $\simeq 5 \times 10^{-3}$ $e$/nm$^2$, which is a reasonable surface charge density. We set the layer thickness $d$ to be equal to the particle diameter $D$, i.e., $d = D$, thus ignoring the effects of colloid immersion in the aqueous phase due to wetting. The dielectric permittivities were taken to be $\varepsilon_w = 80$, $\varepsilon_c = 2.5$, and $\varepsilon_{oil} = 2$ for the water, polystyrene latex beads, and oil (decane or octane) phases, respectively. This represents a good fit in the intermediate ionic strength regime.

In a similar fashion, Figure 6b shows multiple fits to the data in ref 25. The surface pressure was measured for different aging times by varying the exposure time of the monolayer in contact with 250 mM NaCl solution, for 2, 19, and 115 h. As was mentioned in ref 25, the number of dissociated groups on the colloid surface, corresponding to the surface charge, diminishes with time. Hence, Figure 6b shows a decrease in surface pressure with aging time. (Given that the three isotherms
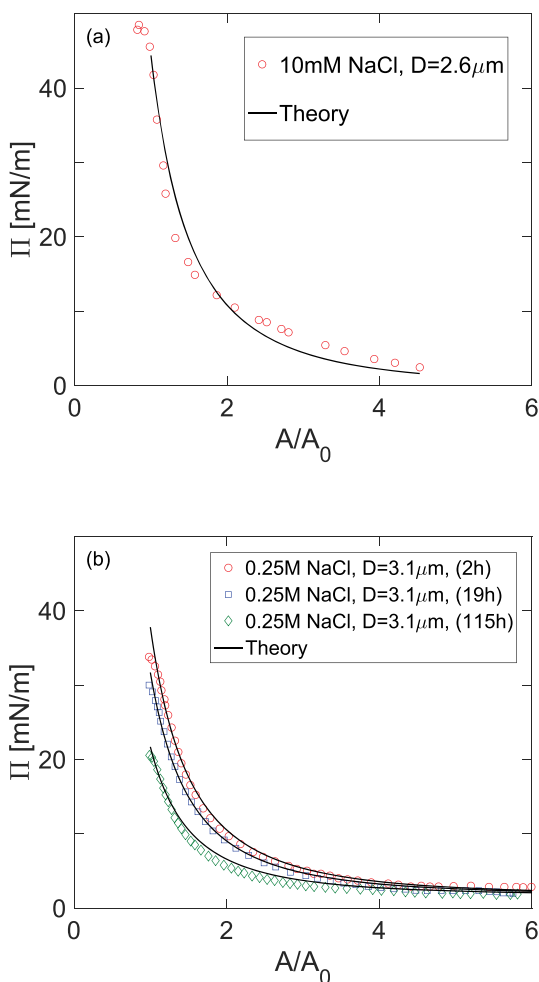
**Figure 6.** Fits of our model to experimental data. (a) Data adapted from Aveyard et al.,[16] with latex particles of radius 1.3 $\mu$m and ionic strength 10 mM spread on the octane/water interface. The fit parameter is $\sigma_a$ = 870 $\mu$C/m$^2$. (b) Data adapted from Vermant et al.,[25] with latex particles of radius 1.5 $\mu$m and ionic strength 250 mM spread on the decane/water interface for different aging times that affect the surface charge. The horizontal axis, $A/A_0 \sim \xi^{-2}$, is the ratio between the measured area, $A$, and its close-packing value, $A_0$. The fit parameter $\sigma_a$ = 720, 650, and 530 $\mu$C/m$^2$ corresponds to aging times of 2, 19, and 115 h, respectively.



**Figure 7.** Power law fit to experimental data in different salt regimes. (a) Data adapted from Vermant et al.[25] The measurements were taken in the close-packing limit and in the high-salt regime, where the DH approximation holds, for aging times of between 2 and 115 h. For all aging times, the expected $A^{-2}$ power law agrees well with the data. (b) Data adapted from Vermant et al.[25] (main figure) and Petkov et al.[17] (inset). Without added salt, a different power law of $(A/A_0)^{-3/2}$ agrees with the data from the same authors (main figure).[25] Measurements performed by Petkov et al. closer to the dilute limit and with no added salt also agree with the $a^{-3/2}$ power law (inset).

approach the same nonzero constant, it seems that there may be a systematic offset in the measurements. We compensate for this offset by introducing into our fit a constant added to the surface pressure. We first fit the 2 h aging time isotherm and obtain a value of 1.7 mN/m for the additive offset. Then, we use this value for the two remaining isotherms.) The colloid diameter was set to $D = 3.1$ $\mu$m, and for aging times of 2, 19, and 115 h, the fits correspond to $\sigma_a$ = 720, 650, and 530 $\mu$C/m$^2$, respectively (charge densities of a few electrons per thousand nm$^2$). As seen in Figure 6, our model yields good agreement with experiments, and the fits become even better for stronger electrolytes (Figure 6b), as one might expect from the DH approximation.

Figure 7a shows measurements made in the strong electrolyte case and mainly in the close-packing regime.[25] The prediction of the close-packing power law, $\Pi \sim a^{-2}$, follows the data points quite well. However, Figure 7b shows that in the absence of salt the measurements made in ref 25 and by Petkov et al.[17] exhibit a different scaling, $\Pi \sim a^{-3/2}$.
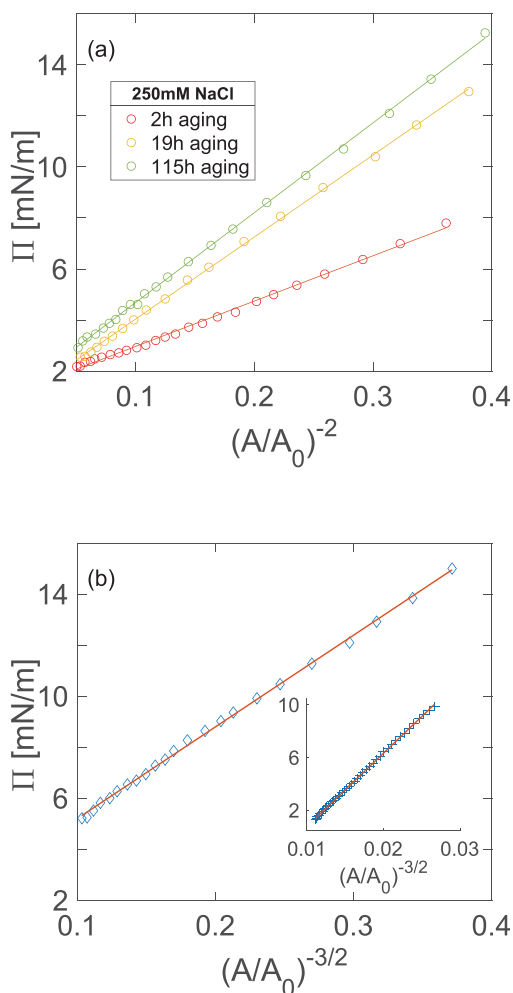
This result is beyond the scope of our model that employs the DH approximation.

## ■ DISCUSSION

Scaling laws derived from the analytical results for the surface free energy and surface pressure are obtained in two limits: (i) the dilute limit ($L \gg D$, Figure 4 and eq 21); (ii) the close-packing limit ($L \to D$, eq 20).

In the dilute limit, we have found that the surface pressure can be described in terms of dipole−dipole interactions, where the effective dipole moment $p_{eff}$, eqs 23 and 24, arises from ionic screening in the aqueous subphase. The charge separation corresponding to this dipole moment, $p_{eff} = p_1 + p_2$, is given in terms of the colloid thickness $d$ for $p_1$ (eq 23) in the strong electrolyte limit or in terms of the Debye screening length for $p_2$ (eq 24) in the weak limit. The sum of these two contributions, $p_1 + p_2$, constitutes the effective dipole moment of each colloid. This description is

valid for intermediate cases and demonstrates an explicit dependence on the monolayer dielectric permittivity and the subphase ionic strength. We note that in previous work[16,33,34] less-general results were derived for the dilute limit, with either $p = p_1$[16] or $p = p_2$ (and only for $Q_a = 0$).[34]

The colloidal monolayer permittivity strongly affects the surface pressure $\Pi$ through the magnitude of $p_1$ (eq 23). The rescaled surface pressure $\Pi/\Pi_0$ of Figure 5 scales as $1/\varepsilon_c$ in the dilute-packing limit, implying that $\Pi \sim 1/\varepsilon_c^2$ (eq 20). However, in the close-packing limit, the rescaled surface pressure is independent of $\varepsilon_c$; hence, $\Pi \sim 1/\varepsilon_c$. The latter observation stems from the difference between the two regimes: dipole–dipole interactions vs a uniform electric double layer.

Several comments can be made on the effects of salt. First, for strong electrolytes, the surface pressure is nearly independent of ionic strength. This result is consistent with experimental findings of a weak dependence of the interparticle force and surface pressure on salt concentration.[16,35] An exception occurs when $Q_w$ and $Q_a$ have opposite signs. For example, in Figure 3, we plot the dependence of $\Pi$ on $\kappa_D$ and show that it is nonmonotonic and even vanishes for a specific salt concentration.

The dependence on salt is quite different for weak electrolytes. A clear divergence of the surface pressure is observed for very weak ionic strength. We remark that eq 25 might be inaccurate in this limit because the validity of the DH approximation breaks down for high surface charges and weak electrolytes. Therefore, it may be more appropriate in this case to consider methods other than the DH approximation.[32,34,36]

We pay special attention to the charge on the water side, $Q_w$. Although it was conveniently set to zero in Figure 6, we find that $Q_w$ can, in certain cases, affect the surface pressure. Because the energetic cost of charging a surface in contact with a low-dielectric material is high, it is commonly believed[17,19,34] that ions from the water phase prefer to diffuse to the air side of the layer. These ions neutralize some of the air-side charges, thus reducing their net charge. As a result, the water-facing charge $Q_w$ can be much higher than $Q_a$.

In contrast to previous theoretical derivations,[16,17,19,35,37] which a priori neglected $Q_w$, we can compare the contributions to the surface pressure from charges located at the top and bottom sides of the monolayer. For example, we calculate separately the surface pressure that results from charges residing only on the colloid/air interface ($\Pi_{ca}$ for $Q_w = 0$) and the opposite case, when they reside only on the colloid/water interface ($\Pi_{cw}$ for $Q_a = 0$). The ratio between them, for each of the scaling limits, is given by

$$\frac{\Pi_{ca}}{\Pi_{cw}} = \left(\frac{Q_a}{Q_w}\right)^2 \left(1 + \frac{\varepsilon_w}{\varepsilon_c}\kappa_D d\right)^\beta \tag{26}$$

where $\beta = 1$ or 2 for the close-packing and dilute regimes, respectively. Clearly, the contribution of the water-side charges cannot be neglected when the surface charge residing on the air side is much smaller than that on the water side. The corresponding $Q_w/Q_a$ ratio in the close-packing regime is estimated to be 10–50 for 1 mM ionic aqueous solution at room temperature and for silica particles of diameter $D = 0.1$–1 $\mu$m. Indeed, this scenario might be achieved in some physical setups.

## ■ CONCLUSIONS

In this work, we study the surface pressure of a monolayer composed of charged colloids at the air/water interface, within the linear PB theory (DH theory). The colloidal monolayer is treated as a continuum dielectric, with dielectric constant $\varepsilon_c$ and finite thickness $d$, separating two phases: an electrolyte solution and air (or oil), with $\varepsilon_w \gg \varepsilon_a$. Charges on the colloidal particles facing the water side and air side are modeled as surface charge patches superimposed on a square lattice. As was previously suggested for similar setups,[22,23] the presence of charged particles at the air/water interface results in excess surface free energy, and the surface pressure can be calculated directly from the latter (eq 11).

Although the exact solution for the surface pressure requires a numerical summation of many terms in eq A7 (Figure 4), the scaling forms are obtained analytically, yielding for the close-packing limit ($\xi = D/L \to 1$), $\Pi \sim \xi^4 \sim a^{-2}$ and for the dilute limit ($\xi \ll 1$), $\Pi \sim \xi^5 \sim a^{-5/2}$. The former is consistent with the uniform surface charge density,[20,23,38] while the latter can be viewed as originating from dipolar interactions between discrete dipoles[16,34] (Appendix B).

The effective dipole moment, $p_{eff}$ of the charged colloids is calculated analytically and is found to depend on the ionic strength (Figure 3), the dielectric properties of the colloidal particles (Figure 5), and the number of charges residing on the water side ($Q_w$) and the air side ($Q_a$) of the colloid. We detail the physical conditions for which the contribution of the water side charges to the surface pressure is not small, in contrast to the common belief. In addition, the dependence on salt concentration is explored. For close-packing and dilute colloid limits, the monolayer permittivity ($\varepsilon_c$) is shown to affect the surface pressure in different ways.

Our model agrees well with available experimental data (Figure 6) using a single fit parameter and explains the physical behavior for strong electrolytes ($\Pi \sim a^{-2}$ in the close-packing limit). However, some experimental results[17,18,25] that exhibit longer-ranged interactions ($\Pi \sim a^{-3/2}$) for weak electrolytes are still poorly understood. Our findings suggest that the latter scaling cannot be obtained within a self-consistent linear theory. This observation contradicts the theoretical model presented in ref 17, where an ansatz of the linear theory was employed to describe experiments outside its range of validity (the no-salt regime). We note that previous theoretical work[20] found the proper scaling in the no-salt regime for *uniform* surface charge to be as strong as $\Pi \sim a^{-1}$, implying that the long-range scaling of the surface pressure might eventually be recovered from a fully nonlinear theory.

We hope that our study, restricted to the DH regime, will stimulate even further theoretical and experimental investigations, which will hopefully shed light on the abnormal surface pressure scaling of charged colloidal monolayers in the no-salt regime.

## ■ APPENDIX A

### Derivation of the Surface Pressure

We derive the solution for the electrostatic potential within the boundary value problem presented in the text. The potential $\tilde{\psi}(\mathbf{k}, z)$ [with $\mathbf{k} = 2\pi/(Ll_{nm})$ and where $l_{nm} = \sqrt{n^2 + m^2}$] in the three spatial regions (with 'a', 'w', and 'c' denoting air, water, and colloid, respectively) is obtained from eqs 12, 13, and 16

$$\tilde{\psi}^{(a)}(\mathbf{k}, z) = \tilde{\psi}_s^{(a)}(\mathbf{k}) \exp(-\Lambda_{nm} z),$$

$$\tilde{\psi}^{(w)}(\mathbf{k}, z) = \tilde{\psi}_s^{(w)}(\mathbf{k}, z) \exp[(\Lambda_{nm}^2 + \kappa_D^2)^{1/2}(z + d)],$$

$$\tilde{\psi}^{(c)}(\mathbf{k}, z) = \tilde{\psi}_s^{(a)}(\mathbf{k}) \frac{\sinh[\Lambda_{nm}(z + d)]}{\sinh(\Lambda_{nm} d)} - \tilde{\psi}_s^{(w)}(\mathbf{k}) \frac{\sinh(\Lambda_{nm} z)}{\sinh(\Lambda_{nm} d)}$$

$$\text{(A1)}$$

with $\Lambda_{nm} \equiv 2\pi\xi l_{nm}/D = 2\pi l_{nm}/L$. By employing the boundary conditions, eq 14, we obtain for the four capacitance matrix elements $C_{ij}^{-1}$ (eq 17)

$$C_{11}^{-1} = \frac{1}{c_{nm}}\left[1 + \frac{\varepsilon_w}{\varepsilon_c}\sqrt{1 + (\kappa_D/\Lambda_{nm})^2}\ \tanh(\Lambda_{nm} d)\right],$$

$$C_{22}^{-1} = \frac{1 + (\varepsilon_a/\varepsilon_c)\tanh(\Lambda_{nm} d)}{c_{nm}},$$

$$C_{12}^{-1} = C_{21}^{-1} = \frac{1}{c_{nm}}\frac{1}{\cosh(\Lambda_{nm} d)}$$

$$\text{(A2)}$$

with $c_{nm}$ above given by

$$c_{nm} = \varepsilon_0\varepsilon_w\Lambda_{nm}\left[\sqrt{1 + (\kappa_D/\Lambda_{nm})^2} + \frac{\varepsilon_a}{\varepsilon_w}\right.$$
$$\left. + \left(\frac{\varepsilon_a}{\varepsilon_c}\sqrt{1 + (\kappa_D/\Lambda_{nm})^2} + \frac{\varepsilon_c}{\varepsilon_w}\right)\tanh(\Lambda_{nm} d)\right]$$

$$\text{(A3)}$$

We now develop the mathematical framework required for the derivation of the surface free energy and pressure. Using the notation $0 \le \xi \equiv D/L \le 1$, we write eq 18 as

$$\langle \Delta f_{el} \rangle \equiv \frac{2\xi^4}{D^4}\sum_{n,m=0}^{\infty} \theta_{nm}(\tilde{\Sigma}C^{-1}\tilde{\Sigma})_{nm}$$

$$\text{(A4)}$$

where $\theta_{nm} = (2 - \delta_{n0})(2 - \delta_{m0})/4$ depends on the Kronecker delta function, $\delta_{nm}$, and where we made use of the square lattice symmetry of our setup. Finally, from eqs 5 and A4, the surface pressure is given by

$$\Pi = \frac{\xi}{2}\frac{d\langle \Delta f_{el} \rangle}{d\xi} - \langle \Delta f_{el} \rangle$$

$$\text{(A5)}$$

The Fourier transform of $s(r)$ in eq 19 has a Gaussian form,

$$\tilde{s}(n\xi, m\xi) = Q\ \exp\left[-\frac{\pi^2}{2}\xi^2 l_{nm}^2\right]$$

$$\text{(A6)}$$

Using this expression, the explicit solution of the electrostatic potential and the capacitance matrix (eqs A1 and A2), we write

$$\langle \Delta f_{el} \rangle = \frac{g(0)}{2}\xi^4 + 2\xi^4\sum_{n=1}^{\infty}g(\xi l_{n0}) + 2\xi^4\sum_{n,m=1}^{\infty}g(\xi l_{nm})$$

$$\text{(A7)}$$

where $g(\rho)$ is a radially symmetric function ($\rho = \xi l_{nm}$) found from eqs A1−A3,

$$g(\rho) = \frac{1}{2\pi D^3\varepsilon_0\varepsilon_w}\frac{1}{\rho h(\rho)}e^{-\pi^2\rho^2}$$

$$\times \left(Q_a^2\left[1 + \frac{\varepsilon_w}{\varepsilon_c}\sqrt{1 + (\kappa_D D/2\pi\rho)^2}\ \tanh(2\pi\rho d/D)\right]\right.$$

$$\left. + Q_w^2\left[1 + \frac{\varepsilon_a}{\varepsilon_c}\tanh(2\pi\rho d/D)\right] + \frac{2Q_a Q_w}{\cosh(2\pi\rho d/D)}\right)$$

$$\text{(A8)}$$

with $h(\rho)$ above defined as

$$h(\rho) = \sqrt{1 + (\kappa_D D/2\pi\rho)^2} + \frac{\varepsilon_a}{\varepsilon_w}$$
$$+ \left(\frac{\varepsilon_a}{\varepsilon_c}\sqrt{1 + (\kappa_D D/2\pi\rho)^2} + \frac{\varepsilon_c}{\varepsilon_w}\right)\tanh(2\pi\rho d/D)$$

$$\text{(A9)}$$

For the analytical derivation of the surface pressure regimes given below, it is sufficient to use $g(\rho)$ and $g'(\rho)$ evaluated at the origin, $\rho = 0$,

$$g(0) = \frac{Q_a^2 d}{\varepsilon_c\varepsilon_0 D^4} + \frac{(Q_a + Q_w)^2}{\varepsilon_0\varepsilon_w\kappa_D D^4}$$

$$\text{(A10)}$$

and

$$g'(0) = -\frac{\varepsilon_a}{\varepsilon_c}\frac{2\pi d^2}{\varepsilon_c\varepsilon_0 D^5}\left[Q_a + \frac{\varepsilon_c}{\varepsilon_w}\frac{Q_a + Q_w}{\kappa_D d}\right]^2$$

$$\text{(A11)}$$

In the close-packing limit, $\Pi$ can be derived analytically by investigating $\langle \Delta f_{el} \rangle$ and its derivative in the $\xi = D/L \to 1$ limit. The dominant contribution to eq A7 originates from the first term because a simple substitution of $\xi \to 1$ in eq A7 implies that the contributions from the two remaining series are exponentially small, approximately on the order of $\exp(-\pi^2) \sim 10^{-5}$, and can be safely neglected. Then, from eqs A7 and A10 one can derive

$$\langle \Delta f_{el} \rangle \simeq \frac{1}{2}\left[\frac{Q_a^2 d}{\varepsilon_c\varepsilon_0} + \frac{(Q_a + Q_w)^2}{\varepsilon_0\varepsilon_w\kappa_D}\right]\frac{\xi^4}{D^4}$$

$$\text{(A12)}$$

Equation 20 is obtained from eqs A5 and A12 and by the substitution $(\xi/D)^4 = L^{-4} = a^{-2}$.

For the dilute limit, $\xi = D/L \ll 1$, we remark that $\langle \Delta f_{el} \rangle$ has the form of a Riemann sum.[39] Following this observation, it can be evaluated in the limit of small $\xi$. For convenience, we express it as (see eq A7)

$$\frac{\langle \Delta f_{el} \rangle}{2\xi^2} = \frac{g(0,0)}{4}\xi^2 + \xi\sum_{n=1}^{\infty}g(n\xi, 0)\xi + \sum_{n,m=1}^{\infty}g(n\xi, m\xi)\xi^2$$

$$\text{(A13)}$$

Here, $g(x, y)$ is a general well-behaved function of two variables. For the one-dimensional sum, we employ the Euler−Maclaurin formula,[39]

$$\sum_{n=1}^{\infty}g(n\xi, 0)\xi = \sum_{k=0}^{\infty}\frac{B_k}{k!}\xi^k\int_0^{\infty}\left.\frac{\partial^k g}{\partial x^k}\right|_{y=0}dx$$

$$\text{(A14)}$$

where $B_k$ represents the Bernoulli numbers, with the first five given by

$$B_0 = 1,\ B_1 = \frac{1}{2},\ B_2 = \frac{1}{6},\ B_3 = 0,\ B_4 = -\frac{1}{30}$$

If $\lim_{x \to \infty} \partial^k g / \partial x^k = 0$ for all $k$, then eq A14 implies that the expansion of $\sum_{n=1}^{\infty} g(n\xi, 0)\xi$ in powers of $\xi$ is

$$\sum_{n=1}^{\infty} g(n\xi, 0)\xi = \int_0^{\infty} g(x, 0)\, \mathrm{d}x - \frac{g(0,0)}{2}\xi - \frac{g'(0,0)}{12}\xi^2 + \dots$$

(A15)

For the double sum, the generalization of the Euler–Maclaurin formula is given by

$$\sum_{n,m=1}^{\infty} g(n\xi, m\xi)\xi^2 = \sum_{j,k=0}^{\infty} \frac{B_j}{j!}\frac{B_k}{k!}\xi^{j+k} \int_0^{\infty}\int_0^{\infty} \frac{\partial^j \partial^k g}{\partial x^j \partial y^k}\, \mathrm{d}x\, \mathrm{d}y$$

(A16)

If $g(x, y)$ has radial symmetry, then it can be written as $g(x, y) = g(\rho)$ where $\rho = \sqrt{x^2 + y^2}$, coinciding with the expression of $g$ in eq A8, where $\rho = \xi l_{nm}$. We can then calculate the double integral in polar coordinates $(\rho, \theta)$ while recalling that $g$ and all of its $\rho$ derivatives should vanish at infinity. These assumptions lead to the following expansion for the double sum,

$$\sum_{n,m=1}^{\infty} g(n\xi, m\xi)\xi^2 = \int_0^{\pi/2}\mathrm{d}\theta \int_0^{\infty} g(\rho)\rho\, \mathrm{d}\rho$$
$$- \xi \int_0^{\infty} g(\rho)\, \mathrm{d}\rho + \frac{g(0)}{4}\xi^2 + \frac{g'(0)}{36}\xi^3 + \dots$$

(A17)

Finally, by substituting eqs A15 and A17 into eq A13, we obtain the expansion of $\langle \Delta f_{\mathrm{el}} \rangle$ for vanishing $\xi$,

$$\langle \Delta f_{\mathrm{el}} \rangle \simeq 2\xi^2 \int_0^{\pi/2}\mathrm{d}\theta \int_0^{\infty} g(\rho)\rho\, \mathrm{d}\rho - \frac{g'(0)}{9}\xi^5$$

(A18)

Using eqs A5, A11, and A18, we obtain the value of $\Pi$ in the dilute limit as

$$\Pi(\xi) = \frac{\pi}{3}\frac{\varepsilon_{\mathrm{a}}}{\varepsilon_{\mathrm{c}}}\frac{d^2}{\varepsilon_{\mathrm{c}}\varepsilon_0}\left[Q_{\mathrm{a}} + \frac{\varepsilon_{\mathrm{c}}}{\varepsilon_{\mathrm{w}}}\frac{Q_{\mathrm{a}} + Q_{\mathrm{w}}}{\kappa_{\mathrm{D}} d}\right]^2 \left(\frac{\xi}{D}\right)^5$$

(A19)

Equation 21 in the text is recovered by substituting $(D/\xi)^2 = a$.

## APPENDIX B

### Surface Pressure and Dipole Interactions for $\xi \ll 1$

We present another way to obtain eqs 21 and 22. We start by considering the interaction energy between two parallel pointlike dipoles of magnitude $p$ at a large separation $L$ that is perpendicular to the dipole direction. The dipoles are placed in the upper half-space with a permittivity of $\varepsilon_{\mathrm{a}}$. Assuming that there is no contribution from the lower half-space (with permittivity $\varepsilon_{\mathrm{w}} \gg \varepsilon_{\mathrm{a}}$), the dipole–dipole interaction energy is[34]

$$u_{\mathrm{int}} = \frac{p^2}{8\pi\varepsilon_{\mathrm{a}}\varepsilon_0 L^3}$$

(B1)

and is equal to one half of the familiar expression for interacting parallel dipoles. Summing over all pairs of parallel dipoles placed on a square lattice embedded in a 3D space, the lattice cohesive energy, $U_c$, is given by

$$U_c = \frac{N}{2}\sum_{\rho_{nm} \neq 0} u_{\mathrm{int}}(\rho_{nm}) \simeq 0.18 N^{5/2}\frac{p^2}{\varepsilon_{\mathrm{a}}\varepsilon_0 A^{3/2}}$$

(B2)

where $\rho_{nm} = L(n, m)$ is an in-plane lattice vector, $N$ the number of particles (and lattice sites), and $A = NL^2$ is the total surface

area. Similar to the derivation of eq 8, we neglect the entropy of the large colloidal particles. Moreover, the entropy of the mobile electrolyte ions approaches the bulk-solution value, which is independent of the area, yielding $U_c = F_{\mathrm{el}} + \mathrm{const}$. In eq B2, we performed a summation over all lattice sites,

$$\sum_{(m,n)\neq(0,0)} \frac{1}{(m^2 + n^2)^{3/2}} \simeq 9.03$$

The surface pressure is then recovered by taking $\Pi = -\mathrm{d}F_{\mathrm{el}}/\mathrm{d}A \simeq -\mathrm{d}U_c/\mathrm{d}A$,

$$\Pi \simeq 0.269 \frac{p^2}{\varepsilon_{\mathrm{a}}\varepsilon_0 a^{5/2}}$$

(B3)

Comparing eq B3 with eq 21, we find that the $p$ value as calculated above is $p = 0.99 p_{\mathrm{eff}}$ for the $p_{\mathrm{eff}}$ in eq 21. Hence, in the dilute limit, eq 22 can be regarded as the effective dipole moment of the colloidal particle.

## ■ AUTHOR INFORMATION

**Corresponding Author**
*E-mail: andelman@post.tau.ac.il.
**ORCID** ⊙
David Andelman: 0000-0003-3185-8475
**Notes**
The authors declare no competing financial interest.

## ■ ACKNOWLEDGMENTS

## ■ REFERENCES

(1) Langmuir, I. The adsorption of gases on plane surface of glass, mica and platinum. *J. Am. Chem. Soc.* **1918**, *40*, 1361−1403.

(2) Blodgett, K. B. Films built by depositing successive monomolecular layers on a solid surface. *J. Am. Chem. Soc.* **1935**, *57*, 1007−1022.

(3) Gaines, G. L. *Insoluble Monolayers at Liquid-Gas Interfaces*; Interscience Publishers: New York, 1966.

(4) Adamson, A. W.; Gast, A. P. *Physical Chemistry of Surfaces*, 6th ed.; Wiley-Interscience: New York, 1997.

(5) Lyklema, J. *Fundamentals of Interface and Colloid Science*; Elsevier: Amsterdam, 2000; Vol. 3.

(6) Binks, B. P.; Horozov, T. S. *Colloidal Particles at Liquid Interfaces*; Cambridge University Press: Cambridge, 2006.

(7) Vogel, N.; Weiss, C. K.; Landfester, K. From soft to hard: the generation of functional and complex colloidal monolayers for nanolithography. *Soft Matter* **2012**, *8*, 4044−4061.

(8) Szekeres, M.; Kamalin, O.; Schoonheydt, R. A.; Wostyn, K.; Clays, K.; Persoons, A.; Dekany, I. Ordering and Optical Properties of Monolayers and Multilayers of Silica Spheres Deposited by the Langmuir-Blodgett Method. *J. Mater. Chem.* **2002**, *12*, 3268−3274.

(9) Krogman, K. C.; Druffel, T.; Sunkara, M. K. Anti-reflective Optical Coatings Incorporating Nanoparticles. *Nanotechnology* **2005**, *16*, S338−S343.

(10) Pieranski, P. Two-Dimensional Interfacial Colloidal Crystals. *Phys. Rev. Lett.* **1980**, *45*, 569−572.

(11) Onoda, G. Direct Observation of Two-Dimensional, Dynamical Clustering and Ordering with Colloids. *Phys. Rev. Lett.* **1985**, *55*, 226−229.

(12) Hurd, A. J.; Schaefer, D. W. Diffusion-Limited Aggregation in Two Dimensions. *Phys. Rev. Lett.* **1985**, *54*, 1043−1046.

(13) Ruiz-Garcia, J.; Gamez-Corrales, R.; Ivlev, B. I. Foam and cluster structure formation by latex particles at the air/water interface. *Phys. A* **1997**, *236*, 97−104.

(14) Reincke, F.; Hickey, S. G.; Kegel, W. K.; Vanmaekelbergh, D. Spontaneous Assembly of a Monolayer of Charged Gold Nanocrystals at the Water/Oil Interface. *Angew. Chem., Int. Ed.* **2004**, *43*, 458−462.

(15) Mbamala, E. C.; von Grünberg, H. H. Charged Colloids and Proteins at an Air-Water Interface: The Effect of Dielectric Substrates on Interaction and Phase Behaviour. *Phys. Rev. E: Stat. Phys., Plasmas, Fluids, Relat. Interdiscip. Top.* **2003**, *67*, 031608.

(16) Aveyard, R.; Clint, J. H.; Nees, D.; Paunov, V. N. Compression and Structure of Monolayers of Charged Latex Particles at Air/Water and Octane/Water Interfaces. *Langmuir* **2000**, *16*, 1969−1979.

(17) Petkov, P. V.; Danov, K. D.; Kralchevsky, P. A. Surface Pressure Isotherm for a Monolayer of Charged Colloidal Particles at a Water/Nonpolar-Fluid Interface: Experiment and Theoretical Model. *Langmuir* **2014**, *30*, 2768−2778.

(18) Petkov, P. V.; Danov, K. D.; Kralchevsky, P. A. Monolayers of Charged particles in a Langmuir Trough: Could Particle Aggregation Increase the Surface Pressure? *J. Colloid Interface Sci.* **2016**, *462*, 223−234.

(19) Bossa, G. V.; Roth, J.; Bohinc, K.; May, S. The Apparent Charge of Nanoparticles Trapped at a Water Interface. *Soft Matter* **2016**, *12*, 4229−4240.

(20) Levental, I.; Janmey, P. A.; Cebers, A. Electrostatic Contribution to the Surface Pressure of Charged Monolayers Containing Polyphosphoinositides. *Biophys. J.* **2008**, *95*, 1199−1205.

(21) Biesheuvel, P. M.; van Soestbergen, M. Counterion volume effects in mixed electrical double layers. *J. Colloid Interface Sci.* **2007**, *316*, 490−499.

(22) Andelman, D.; Brochard, F.; Joanny, J. F. Phase Transitions in Langmuir Monolayers of Polar Molecules. *J. Chem. Phys.* **1987**, *86*, 3673−3681.

(23) Hachisu, S. Equation of State of Ionized Monolayers. *J. Colloid Interface Sci.* **1970**, *33*, 445−454.

(24) Bakker, G. Kapillarität und Oberflächenspannung. *Handbuch der Experimentalphysik, Band 6*; Akademische Verlagsgesellschaft: Leipzig, 1928.

(25) Reynaert, S.; Moldenaers, P.; Vermant, J. Control over Colloidal Aggregation in Monolayers of Latex Particles at the Oil-Water Interface. *Langmuir* **2006**, *22*, 4936−4945.

(26) Markovich, T.; Andelman, D.; Podgornik, R. Surface tension of electrolyte solutions: A self-consistent theory. *EPL* **2014**, *106*, 16002.

(27) Markovich, T.; Andelman, D.; Podgornik, R. Surface tension of electrolyte interfaces: Ionic specificity within a field-theory approach. *J. Chem. Phys.* **2015**, *142*, 044702.

(28) Andelman, D. Electrostatic Properties of Membranes: The Poisson-Boltzmann Theory. *Handbook of Biological Physics*; Elsevier Science B.V.: Amsterdam, 1995.

(29) Markovich, T.; Andelman, D.; Podgornik, R. Charged Membranes: The Poisson-Boltzmann Theory, DLVO Paradigm and Beyond. In *Handbook of Lipid Membranes*; Safinya, C., Raedler, J., Eds.; Taylor and Francis, 2018.

(30) Verwey, E. J. W.; Overbeek, J. Th. G. *Theory of the Stability of Lyophobic Colloids: The Interaction of Sol Particles Having an Electric Double Layer*; Elsevier: Amsterdam, 1948.

(31) Ben-Yaakov, D.; Andelman, D.; Diamant, H. Interaction between heterogeneously charged surfaces: Surface patches and charge modulation. *Phys. Rev. E* **2013**, *87*, 022402.

(32) Frydel, D.; Oettel, M.; Dietrich, S. Charge renormalization effects in the electrostatic interactions of colloids at interfaces. *Phys. Rev. Lett.* **2007**, *99*, 118302.

(33) Hurd, A. J. The Electrostatic Interaction between Interfacial Colloidal Particles. *J. Phys. A: Math. Gen.* **1985**, *18*, L1055−L1060.

(34) Oettel, M.; Dietrich, S. Colloidal Interactions at Fluid Interfaces. *Langmuir* **2008**, *24*, 1425−1441.

(35) Aveyard, R.; Binks, B. P.; Clint, J. H.; Fletcher, P. D. I.; Horozov, T. S.; Neumann, B.; Paubov, V. N. Measurement of Long-Range Repulsive Forces between Charged Particles at an Oil-Water Interface. *Phys. Rev. Lett.* **2002**, *88*, 246102.

(36) Park, B. J.; Pantina, J. P.; Furst, E. M.; Oettel, M.; Reynaert, S.; Vermant, J. Direct measurements of the effects of salt and surfactant on interaction forces between colloidal particles at water-oil interfaces. *Langmuir* **2008**, *24*, 1686−1694.

(37) Uppapalli, S.; Zhao, H. The Influence of Particle Size and Residual Charge on Electrostatic Interactions between Charged Colloidal Particles at an oil-water interface. *Soft Matter* **2014**, *10*, 4555−4560.

(38) Davies, J. T. The Distribution of Ions Under a Charged Monolayer, and a Surface Equation of State for Charged Films. *Proc. R. Soc. London, Ser. A* **1951**, *208*, 224−247.

(39) Abramowitz, M., Stegun, I. A., Eds.; *Handbook of Mathematical Functions, with Formulas, Graphs, And Mathematical Tables*, 10th ed.; Dover Publications: New York, 1972.